Engineered Science
DOI: https://dx.doi.org/10.30919/es1446

Excel Modeling and Performance Evaluation of Solar Still: Comprehensive Analysis

Pankaj Dumka,[1,*] Rishika Chauhan,[2] Sonawane Chandrakant,[3, 13] Choon Kit Chan,[4,*] Feroz Shaik,[5] Ghanshyam G Tejani,[6, 7] Subhav Singh[8, 9, 10] and Deekshant Varshney[11, 12]

Abstract

Water scarcity is a pressing issue worsened by population growth and industrialization, necessitating efficient and sustainable water purification methods. Conventional solar still (CSS) offers a promising solution but suffers from low productivity and large area requirements. To address these limitations, this study explores the use of Microsoft Excel as a tool for modeling the performance of a conventional solar still. Through Excel, complex thermal processes involved in solar distillation can be simulated and analyzed, aiding in design optimization and performance evaluation. This paper presents a detailed algorithm for modeling CSS in Excel, utilizing Dunkle's semi-empirical relations to predict distillate yield. Visual Basic applications (VBA) functions are developed to automate property evaluations and heat transfer calculations. Experimental data from a CSS setup are used to validate the model, demonstrating a decent agreement between theoretical predictions and experimental results, as listed in the literature. It has been observed that the distillate output and efficiency of the solar still, as predicted by the model proposed by Dunkel, show variations of 16% and 19% from the experimental results. These variations are acceptable, as stated in the literature as well. Overall, Excel modeling proves to be a user-friendly and versatile tool for modeling solar stills.

Keywords: Microsoft Excel; Solar still; Desalination; Dunkle model; Spreadsheets; Energy efficiency.
Received: 10 December 2024; Revised: 01 January 2025; Accepted: 11 January 2025.
Article type: Research article.

1. Introduction

Solar energy is considered one of the most important renewable energy sources, and it can be used in many ways.[1] With excessive population growth and tremendous industrialization, potable water is becoming increasingly scarce with every passing day. Therefore, engineers and scientists have come up with several water purification and filtration methods and devices.[2] The problem with these devices is their large capital investment, involved maintenance, a handsome amount of energy requirements, and also requires skilled operators. Hence, they are not a good fit for poor economies around the globe. To overcome these difficulties, researchers have started focusing on purification methods that are not only environmentally friendly but also economical and sustainable. Solar still, which is also called a conventional solar still (CSS), is one such device that perfectly fits into this category.[3,4] CSS is a cavity with a trapezoid cross section in which brackish water is fed, and the cavity is covered from the top with the help of a thin transparent glass. When sun rays fall on it, due to the greenhouse effect, the evaporation rate of water increases, and the vapor moves to the inner surface of the glass. Here, they release their latent heat and condense. The condensate is then collected and can be used for drinking purposes.[5,6]

The only drawback of this device is its low yield and large area requirement. Thus, the scientific community is striving

[1] *Department of Mechanical Engineering, Jaypee University of Engineering and Technology, A.B. Road, Raghogarh, Guna, Madhya Pradesh, 473226, India*
[2] *Department of Electronics and Communication Engineering, Jaypee University of Engineering and Technology, A.B. Road, Raghogarh, Guna, Madhya Pradesh, 473226, India*
[3] *Symbiosis Institute of Technology, Symbiosis International Deemed University, Pune, 412115, India*
[4] *Faculty of Engineering and Quantity Surveying, INTI International University, Nilai, Negeri Sembilan, 71800, Malaysia*
[5] *Department of Mechanical Engineering, College of Engineering, Prince Mohammad Bin Fahd University, Al Khobar, 31952, Saudi Arabia*
[6] *Department of Research Analytics, Saveetha Dental College and Hospitals, Saveetha Institute of Medical and Technical Sciences, Saveetha University, Chennai, 600077, India*

hard to increase its productivity and efficiency. Several experimental studies have been reported in the past to enhance the productivity of CSS.[7–9] Apart from this, researchers have also given some numerical or empirical results to predict the performance of CSS or modified CSS. In this list, some benchmark studies have been done by Dunkle,[10] Clark,[11] Agarwal and Tiwari,[12] Spalding,[13] and Tsilingiris.[14,15] In all these, the first and the most used work is that of Dunkle. He gave some semi-empirical relations to predict the convective and evaporative heat transfer coefficients, based on which the yield is predicted. Ghachem *et al*.[16] conducted a numerical study on 3D double-diffusive natural convection in an inclined solar distiller, solving the governing equations with the help of the finite volumes method to optimize the distiller's inclination for maximum mass and heat transfer at a fixed Rayleigh number of 10^5. The study examines the effects of buoyancy ratio and inclination for opposed temperature and concentration gradients. Younis *et al*.[17] present a comprehensive review of recent advancements in various solar still types, highlighting key findings and improvements in the basin absorption and productivity through materials and additional systems. They offer a detailed overview of theoretical, experimental, and computational studies, summarizing key results in a useful table to guide future research in the field. Attia *et al*.[18] investigated the effects of TiO_2 nano-coated basin and glass cover cooling at different concentrations on a traditional hemispherical solar still (HSS) in El Oued City, Algeria. Younis *et al*.[19] reviewed the effectiveness of HSS for addressing freshwater shortages, emphasizing their superior thermal performance compared to other solar still types. The review compiles key findings on design, operation, efficiency, yield, and cost analysis, providing a comprehensive guide for future research on enhancing HSS performance.

In most cases, the newcomer to the field of solar water desalination has to learn programming languages, such as MATLAB or Python, to program the relations and plot the result, which takes a huge amount of time.[20] Moreover, MATLAB is not an open-source package (freely available for use). Therefore, one should have a tool that is not only easily available but also has the capability of performing simple to complex programming and graphing. Here comes the importance of Microsoft Excel, which every Windows user has or can easily access on other operating systems.[21] Therefore, Excel modelling emerges as a valuable tool for researchers, educators, and practitioners alike.

Excel modelling offers a versatile platform for simulating and analyzing complex thermal processes.[22,23] Through Excel, users can construct mathematical models that simulate various parameters to understand and feel the dynamics of heat transfer within the solar still cavity.[24,25] Thus, the users can explore different design configurations and operating conditions to optimize the water production efficiency. Moreover, Excel facilitates the visualization of data through graphs, charts, and tables, thus enabling users to interpret and communicate their findings effectively. This visual representation enhances understanding and facilitates decision-making regarding solar still design, operation, and performance evaluation.[26,27]

One of the key advantages of Excel modelling is its user-friendly interface, which makes it accessible to a wide range of users with varying levels of technical expertise. Excel's familiar spreadsheet layout allows users to input data, define equations, and perform calculations using intuitive functions and formulas. Additionally, Excel's built-in features, such as conditional formatting, data validation, and pivot tables, streamline the modelling process and enhance productivity. Furthermore, Excel supports the integration of visual basic for applications (VBA) macros, thereby enabling users to automate repetitive tasks, customize functionalities, and extend the capabilities of their models.[28] This flexibility empowers users to tailor their Excel-based simulations to suit specific research objectives or educational goals.

Hence, the objective of this article is to show the readers how a simple Excel modelling can serve as a valuable resource for enhancing the understanding of solar distillation, which can advance the development of sustainable water solutions. It has been shown in this article that Excel's ease of use, compatibility, and analytical capabilities can make it an indispensable tool for researchers, educators, and practitioners striving to address global water challenges.

In this article, a detailed algorithm has been presented on how to model CSS and its application in Excel. The Dunkle model has been used to predict the distillate yield based on the pertinent input variables. Functions for different parameters have been written in VBA and are presented in the article for the reader to use them and start their journey in the domain of thermal modelling of solar still using Microsoft Excel. To understand the data generated by the Microsoft Excel, visual aid of Excel has been used, viz. the plots are drawn using 'Scatterplot' function of Excel. At last, the results obtained from the analysis have been discussed, followed by the

[7] *Applied Science Research Center, Applied Science Private University, Amman, 11931, Jordan*
[8] *Chitkara Centre for Research and Development, Chitkara University, Himachal Pradesh, 174103, India*
[9] *Division of research and development, Lovely Professional University, Phagwara, Punjab, 144411, India*
[10] *Centre for Promotion of Research, Graphic Era (Deemed to be University), Uttarakhand, Dehradun, 248002, India*
[11] *Centre of Research Impact and Outcome, Chitkara University, Rajpura, Punjab, 140417, India*
[12] *Division of Research & Innovation, Uttaranchal University, Dehradun, 248007, India*
[13] *Symbiosis Centre for Nanoscience and Nanotechnology, Symbiosis International Deemed University, Pune, 412115, India*
**Email:*p.dumka.ipec@gmail.com (P. Dumka);
choonkit.chan@newinti.edu.my (C. K. Chan)

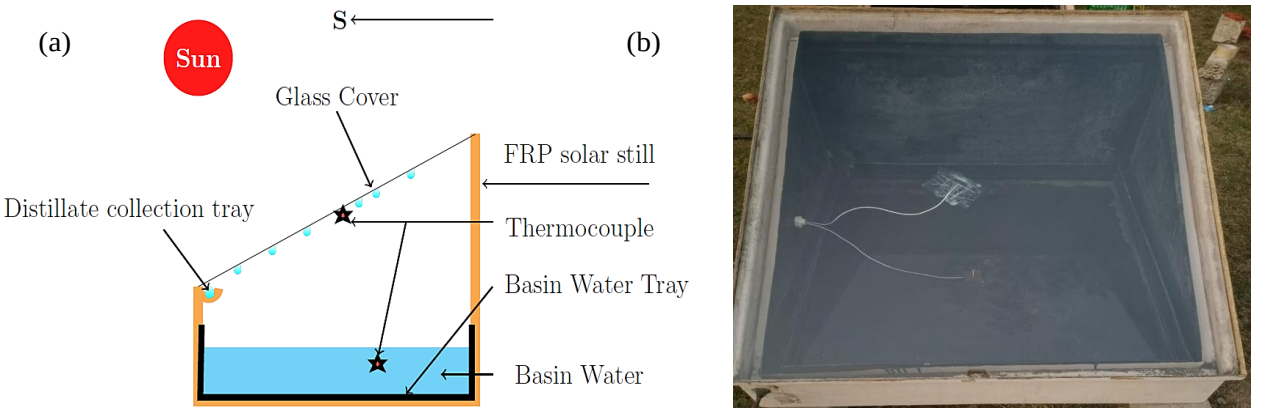

Fig. 1: CSS (a) Schematic diagram and (b) Actual photograph.[15]

conclusion.

2. Experimentation and uncertainty

To conduct the experimentation, two CSS constructed from 5 mm-thick fiberglass reinforced plastic (FRP) were utilized. The shorter side wall of the still measures 19.5 cm, while the longer side measures 64.5 cm. A transparent iron glass, 4 mm thick, was employed to enclose the still cavity. To ensure no vapour leakage from the sides of the glass, Putty (clay) has been applied on the top edges of the glass cover and CSS. The glass cover is inclined at an angle of 24° from the ground level to optimize the absorption of sunlight. Additionally, a black-painted Galvanized Iron (GI) tray, with a thickness of 0.74 mm, was used to contain the basin water. The base area of the tray is 1 square meter. Figs. 1(a) and (b) show the schematic representation and actual photo of CSS, respectively.

Distillate collection occurred on an hourly basis, utilizing a graduated cylinder for measurement accuracy. Concurrently, solar radiation intensity was monitored using a solar-powered meter (TM-207). The solar-powered meter was calibrated before the experiments and was positioned to match the angle of the glass cover. The basin water, inner glass cover, and ambient air temperatures were measured and recorded every hour, with the help of calibrated k-type thermocouples and MDTI1039T digital temperature indicator.

The collected data were logged and analyzed by using Microsoft Excel. The temperature readings were used to calculate the thermophysical properties of moist air, heat transfer coefficients, and thermal efficiency of the CSS, while the distillate yield was compared to the predictions made by Dunkle's semi-empirical model.

Recognizing uncertainty leads to questioning the reliability of a quantification result, indicating its precision. Without stating the associated uncertainty, the result, assumed to be the true value, is incomplete. Table 1 specifies detailed information on the operating ranges, accuracies (a), and standard uncertainties (u) of the instruments that were engaged in the measurements. The relation between u and a is given as follows in Eq. (1):[29]

$$u = a/\sqrt{3} \quad (1)$$

Table 1: a, range, and u of the measuring devices.

Instrument	a	Range	u
Graduated cylinder (mL)	± 1	0–250	0.6
Thermocouple (°C)	± 0.1	-100–500	0.06
Solarimeter (W m^{-2})	± 10	0–1999	5.77

The uncertainty associated with a measured quantity (y) that depends on input parameters (x_i) is determined using Eq. (2).[30]

$$u(y) = \sqrt{\left(\frac{\partial y}{\partial x_1}\right)^2 \times u^2(x_1) + \left(\frac{\partial y}{\partial x_2}\right)^2 \times u^2(x_2) + \cdots} \quad (2)$$

Following Eq. (2), the uncertainty related to the solar still's efficiency is calculated by utilizing Eq. (3).

$$u(\eta) = \sqrt{\left(\frac{L}{IA_s}\right)^2 \times u^2(\dot{m}_{ew}) + \left(\frac{1}{IA_s}\right)^2 \times u^2(I)} \quad (3)$$

As calculated from Eq. (3), the highest uncertainty in the efficiency of the solar distiller unit is about 1.99%.

The experiments were conducted during the month of September 2023 at JUET, situated in Raghogarh, Guna, Madhya Pradesh, India (24°26′07″N, 77°09′39″E). Consistently, throughout the investigative research, the basin water was maintained at a constant weight of 30 kg. The following key variables were carefully recorded on an hourly basis:

- Basin water, inner glass, and surrounding atmosphere temperatures
- Intensity of solar radiation.
- Distillate output

3. Solar still mathematics and VBA functions

When performing solar still design calculations, the first thing to evaluate is the thermophysical properties of the moist air. The properties used in this article are the one proposed by Toyama.[31] The thermophysical properties are summarized in Table 2. T_v represents the average temperature between water and glass, *i.e.*, $(T_w + T_{ci})/2$.

To automate the task of property evaluation, in Excel, the properties are written as functions in VBA. These functions

Table 2: Thermophysical properties of moist air.[32]

Symbol	Quantity	Expression
c_p	Specific heat at constant pressure	$999.2 + 0.1434T_v + 1.101 \times 10^{-4}T_v^2 - 6.7581 \times 10^{-8}T_v^3$
ρ	Moist air density	$353.44/(T_v + 273.15)$
k	Thermal conductivity	$0.0244 + 0.7673 \times 10^{-4}T_v$
μ	Dynamic viscosity	$1.718 \times 10^{-5} + 4.62 \times 10^{-8} \times T_v$
L	Latent heat	For $T_v \geq 70$ °C: $3.1615 \times 10^6(1 - 7.616 \times 10^{-4}T_v)$ For $T_v < 70$ °C: $2.4935 \times 10^6(1 - 9.4779 \times 10^{-4}T_v + 1.3132 \times 10^{-7}T_v^2 - 4.974 \times 10^{-9}T_v^3)$
p_w	Partial saturated vapour pressure at water temperature	$e^{\left(25.317 - \frac{5144}{T_w + 273.15}\right)}$
p_{ci}	Partial saturated vapour pressure at inner glass temperature	$e^{\left(25.317 - \frac{5144}{T_{ci} + 273.15}\right)}$
β	Volumetric expansivity	$\frac{1}{T_v + 273.15}$

are presented in Table S1. To call these functions, one can simply write the function name after "=" and then pass the appropriate arguments (numerical values or references to the numerical values), as shown in Fig. S1. In this case, the specific heat is evaluated at the mean temperature of 10 °C.

As in the still cavity, the vapours rise due to the natural convection, so the pertinent nondimensional numbers governing the flow are Nu (Nusselt number), Pr (Prandtl number), and Gr (Grashof number), which are defined in Eqs. (4)-(6), respectively.[33,34]

$$\mathrm{Nu} = \frac{h_{cw} d}{k} \tag{4}$$

$$\mathrm{Pr} = \frac{\mu c_p}{k} \tag{5}$$

$$\mathrm{Gr} = \frac{g \times \beta \times d^3 \times \rho^2 \times \Delta T}{\mu^2} \tag{6}$$

where h_{cw}, d, k, μ, c_p, g, β, ρ, and ΔT are the convective heat transfer coefficient, characteristic dimension of still, thermal conductivity of vapour, dynamic viscosity, specific heat of vapur, acceleration due to gravity, volumetric expansivity, density of vapour, and temperature difference between water and glass.

The Excel VBA functions to evaluate Pr and Gr are presented in Table S2. The relation between these variables is shown in Eq. (7).[33]

$$Nu = \frac{h_{cw} d}{k} = f(Gr \times Pr) \tag{7}$$

Dunkle was the first person to give the semi-empirical relation to obtain the value of h_{cw}, based on his indoor experiments. His formula is independent of d (the characteristic dimension of the solar still). The model to evaluate the h_{cw} and the corresponding convective heat transfer rate are shown in Eqs. (8) and (9), respectively.[10]

$$h_{cw} = 0.884 \times \left(T_w - T_{ci} + \frac{(p_w - p_{ci})(T_w + 273.15)}{(268.9 \times 10^3 - p_w)}\right)^{1/3} \tag{8}$$

$$q_{cw} = h_{cw} \times (T_w - T_{ci}) \tag{9}$$

where T_w, T_{ci}, p_W, and p_{ci} are the water temperature, inner condensing temperature, partial pressure of water from the basin surface, and partial pressure of water at the inner condensing cover. The Excel VBA function to evaluate h_{cw} is shown in Table S3.

After h_{cw}, the next step is to evaluate the evaporative heat transfer coefficient (h_{ew}) and rate (q_{ew}). These values are evaluated with the help of Eqs. (10) and (11), respectively.[35] The Excel VBA function to solve for h_{ew} is shown in Table S4.

$$h_{ew} = 0.0167273 \times h_{cw} \times \left(\frac{p_w - p_{ci}}{T_w - T_{ci}}\right) \tag{10}$$

$$q_{ew} = h_{ew} \times (T_w - T_{ci}) \tag{11}$$

The point to note here is that both convective and radiative heat transfers are coupled, but the radiative heat transfer is the independent mode of heat transfer from water to the inner condensing cover, as it depends only on the temperatures, not the medium of heat transfer. The radiative heat transfer coefficient (h_{rw}) and rate (q_{rw}) from water to the glass surface are evaluated using Eqs. (12) and (13), respectively.[32]

$$h_{rw} = \left(\frac{1}{\varepsilon_g} + \frac{1}{\varepsilon_w} - 1\right)^{-1} \times F_{12} \times \sigma \times \left(\frac{(T_w + 273.15)^4 - (T_{ci} + 273.15)^4}{T_w - T_{ci}}\right) \tag{12}$$

$$\dot{q}_{rw} = h_{rw} \times (T_w - T_{ci}) \tag{13}$$

where ε_g, ε_w, F_{12}, and σ are the emissivity of glass, emissivity of water, view factor from water to glass, and Stefan-Boltzmann constant (5.67×10^{-8} W/m^{2}K^4). In the analysis, it is considered that $\varepsilon_g = \varepsilon_w = 0.9$ and $F_{12} = 1$. The Excel VBA function to evaluate h_{rw} is shown in Table S5.

To know the influential mode of heat transfer within the

solar still, energy fractions are evaluated. First, the overall heat transfer coefficient (h_{1w}) and rate ($\dot{q}_{1w}$) are evaluated with the help of Eqs. (14) and (15).[32]

$$h_{1w} = h_{cw} + h_{ew} + h_{rw} \quad (14)$$

$$\dot{q}_{1w} = h_{1w} \times (T_w - T_{ci}) \quad (15)$$

Thereafter, the energy fractions, viz., convective, evaporative, and radiative fractions, are evaluated, with the help of Eqs. (9), (11), (13), and (15) as shown in Eqs. (16)-(18).[32]

$$F_{cw} = \frac{\dot{q}_{cw}}{\dot{q}_{1w}} \quad (16)$$

$$F_{ew} = \frac{\dot{q}_{ew}}{\dot{q}_{1w}} \quad (17)$$

$$F_{rw} = \frac{\dot{q}_{rw}}{\dot{q}_{1w}} \quad (18)$$

The theoretical distillate output is obtained by dividing q_{ew} by the latent heat of vaporization (L), as shown in Eq. (19).[32]

$$\dot{m}_{ew} = \frac{\dot{q}_{ew}}{L} \quad (19)$$

Finally, the instantaneous efficiency of the solar still is evaluated with the help of Eq. (20).[36]

$$\eta_i = \frac{\dot{m}_{ew} \times L}{A_s \times I \times 3600} \quad (20)$$

where A_s is the surface area of water, which in our case is 1 m^2, and I is the solar radiation intensity.

4. Implementation of functions and Excel calculations

First, the experimental data is stored in the Excel file under the heading "Input Data", as shown in Fig. S2. Here, 'Ta' and 'm_exp' are the atmospheric temperature and the distillate yield obtained during the experimentation. Then, make a heading "Calculations", where the final calculations will be done. Under this heading, select 15 columns for the evaluation of hcw, hew, hrw, h1w, qcw, qew, qrw, q1w, Fcw, Few, Frw, L, m_th, ηi_th, ηi_exp. Here, the "_th" and "_exp" stand for the theoretical and experimental, respectively. The header of the Calculations is shown in Fig. S3.

The solution strategy will be such that, first, the full first row, *i.e.*, the one corresponding to 9:00 h, will be solved. Thus, in this regard, first hcw, hew, and hrw will be evaluated based on the developed functions, as shown in Fig. S4. Then, h1w, qcw, qew, qrw, and q1w will be evaluated based on Eqs. (9), (11), (12) and (15), respectively. Fig. S5 shows the formulas and numerical values.

Thereafter, energy fractions will be evaluated based on the Eqs. (16)-(18) and the latent heat will be evaluated based on the developed function. Then, the theoretical distillate output will be evaluated based on Eq. (19). Once the theoretical distillate is known, the theoretical efficiency is evaluated, and the experimental efficiency is evaluated with the help of obtained experimental distillate yield. Both the efficiencies are evaluated with the help of Eq. (20). The formulas and numerical values are shown in Fig. S6. Once this is done, the first, full row of calculations, *i.e.*, the calculations for 9:00 h can be seen in Fig. S7. Then, the task is simply to select the first row and drag it till 21:00 h. The full final output can is seen in Fig. S8. Now one can observe that, in the efficiency column the erroneous values start coming after 16:00 h, which even reaches to a NAN (not a number), this is due to the sharp reduction in the solar radiation intensity after 16:00 h which reaches a zero mark after 18:00 h (refer Fig. 3).

5. Results and discussion

Fig. 2 shows the variation of solar radiation intensity and ambient temperatures with respect to time. The solar radiation at the beginning of the experiments was 575 W/m^2, and the corresponding ambient temperature was 19.5 °C. As the day progresses, it increases to a maximum value of 1000 W/m^2, which gradually reduces to zero by 19:00 h. The peak surrounding temperature recorded was 37 °C, whereas the average temperature during the experiment was close to 28 °C.

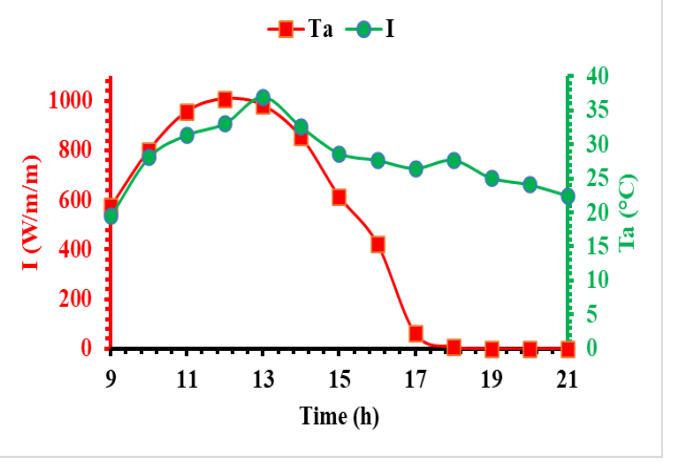

Fig. 2: Variation of solar radiation intensity and ambient temperature.

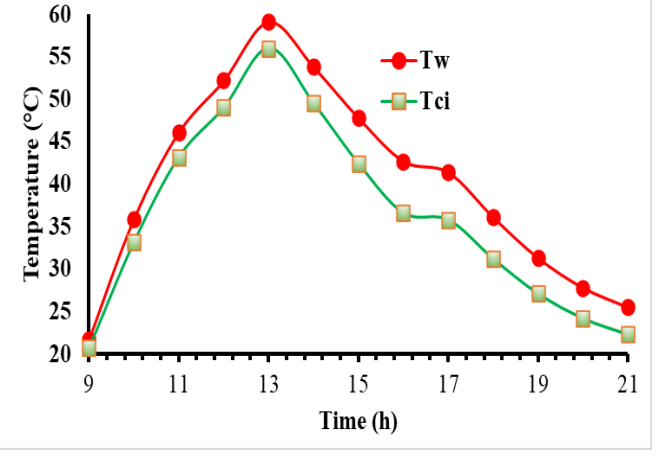

Fig. 3: Variation of basin water and inner condensing temperatures.

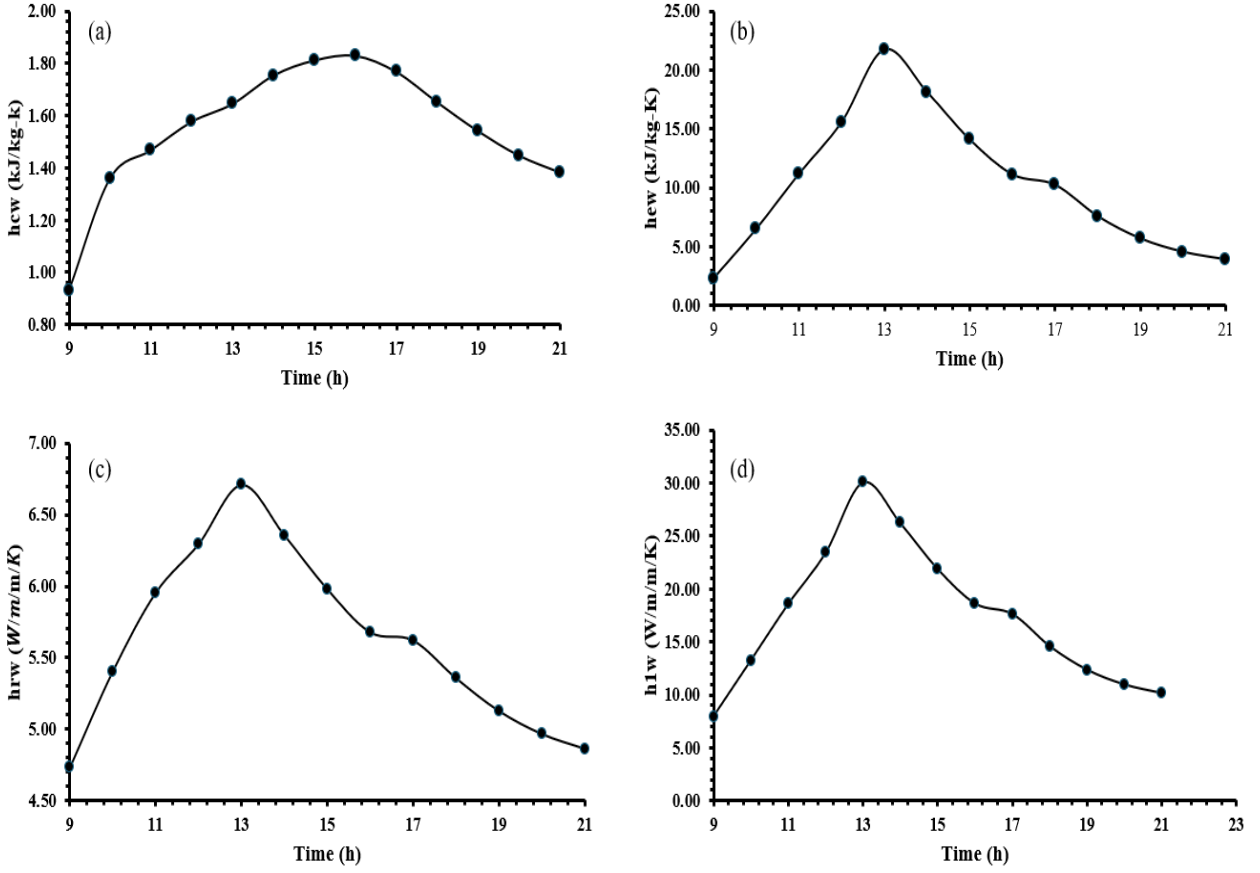

Fig. 4: Variation of different heat transfer coefficients. (a) convective heat transfer coefficient, (b) evaporative heat transfer coefficient, (c) radiative heat transfer coefficient, and (d) overall heat transfer coefficient.

Fig. 3 shows the variation of recorded T_w and T_{ci} during the experiment. At the start of the experiment, the temperature difference between water and glass is very close, as the radiation is not that strong in the morning hours. As the day progresses, both the temperature increases and at 13:00 h, the water temperature is 5.54% higher than the glass. The highest temperature difference of 16.7% is observed at 16:00 h.

The variation of the h_{cw} as obtained from Dunkle's model is shown in Fig. 4(a). It shows that at the experimental h_{cw} was 0.93 W/m^2-K, which sharply increased to 1.36 W/m^2-K, and then the rate of increase reduced. The maximum value of h_{cw} was 1.83 W/m^2-K at 16:00 h, viz. 96.8% higher than the start of the experiment. This is due to the maximum temperature difference between water and the inner condensing cover temperature at 16:00 h. Thereafter, it reduces and at the end of the experiment attains a value of 1.38 W/m^2-K.

The variation of h_{ew} as a function of time is shown in Fig. 4 (b). One can observe that there is a continuous rise in the value of h_{ew} till 13:00 h, and then it reduces. This behaviour is due to the rise in the temperature difference between water and glass, which will result in an increase in the distillate output in this period. The higher the h_{ew}, the more the distillate output. In comparison to the start of the experiment, the value of h_{ew} at 13:00 h is 858 and 460% higher than its value at the start and the end of the experiment, respectively. One more observation is that the rise in the value of hew has a steeper slope than its fall. This is due to the large specific heat of water, which is not allowing the water to cool down fast, even in poor or no sunlight.

The variation of h_{rw} is shown in Fig. 4 (c). It can be observed that h_{rw} rises to a maximum value and then decreases. The reason is that, as time increases, the temperature difference between water and glass rises, and attains a maximum value at the peak radiation hour, thereafter it reduces. Here, one can see that the maximum value is again at 13:00 h. This is obvious, as h_{rw} relies on the Stefan-Boltzmann law, which depends on temperature, and the highest temperature difference is obtained at 13:00 h. The peak value of h_{rw} leads its start and end values by 42 and 38%, respectively.

Fig. 4 (d) shows the variation of h_{1w}, which is the sum of all the heat transfer coefficients discussed previously. Therefore, it is totally influenced by the magnitude of the highest heat transfer coefficient among all the heat transfers, which is nothing but h_{ew}. To further stem this fact, one can also see Fig. 5, which shows the fraction of energy taken up by the evaporative, convective, and radiative heat transfer rates from water to glass. The plot illustrates that convective heat transfer is the least powerful mode, followed by radiative, with evaporative being the most effective. During one hour in the morning and one hour in the evening, radiative heat

transfer is higher, while evaporative heat transfer leads the rest of the time. This pattern occurs because the solar radiation is typically weak or absent during those hours, resulting in lower evaporation rates and, accordingly, reduced evaporative heat transfer.

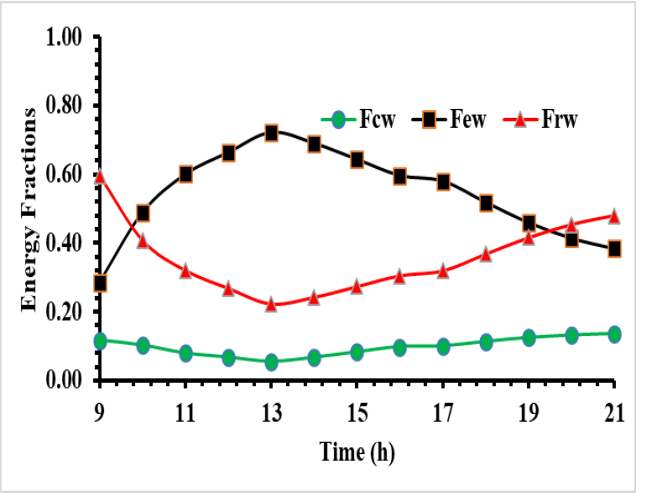

Fig. 5: Variation of energy fractions.

The variation of the theoretical and experimental distillate output from the solar still is shown in Fig. 6. In the morning and the evening hours, the distillate predicted by Dunkle's model is close to the experimental result. Whereas in the mid-time, *i.e.*, peak radiation hours, where the temperature inside the still becomes higher, it tends to deviate. This is because Dunkle's model works best in the operating and mean temperature range of 17 and 50 °C, respectively. At 9:00 h, the theory predicts 66% lower results than the experimental. This difference then decreases to 8% by 11:00 h. Thereafter, the experimental yield takes the lead over theoretical and maintains it throughout the experiment. At 14:00 h, the distillate obtained experimentally is 16% higher than the theoretical. Overall, the cumulative distillate yield from CSS is 972 mL experimentally and 810 mL theoretically.

The theoretical model, based on Dunkle's semi-empirical relations, predicts a distillate output that is 16% lower than the experimental results. This difference indicates that, while the model provides a close approximation, it tends to slightly underpredict the actual performance of the CSS. However, this variation is consistent with the findings reported in the literature, where similar deviations have been observed.[37,38] This alignment with previously published results suggests that the model is valid and reliable within the acceptable error margins. The comparison of the theoretical predictions with the experimental data serves as a validation step, confirming that the model captures the key dynamics of the solar distillation process and provides a reasonable estimate of the distillate yield. This validation process demonstrates that the model, despite its simplified assumptions, can effectively simulate real-world performance, making it a valuable tool for further analysis and optimization of CSS designs.

The variation of experimental and theoretical instantaneous efficiency of CSS as a function of time is shown in Fig. 7. The data till 16:00 h is shown, as after this time the solar radiation intensity reduces very sharply to zero value, which results in impractical results. Both theoretically and experimentally, the efficiency increases with increasing time as the distillate increases. Moreover, as the theoretical distillate is lower than the experimental (after 11:00 h), the theoretical efficiency value is lower than the experimental. Overall, the experimental efficiency of CSS is 19% higher than that of the theoretical.

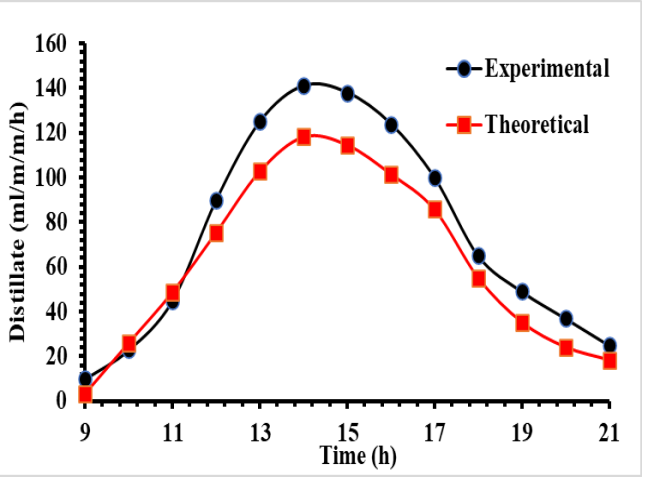

Fig. 6: Variation of distillate output.

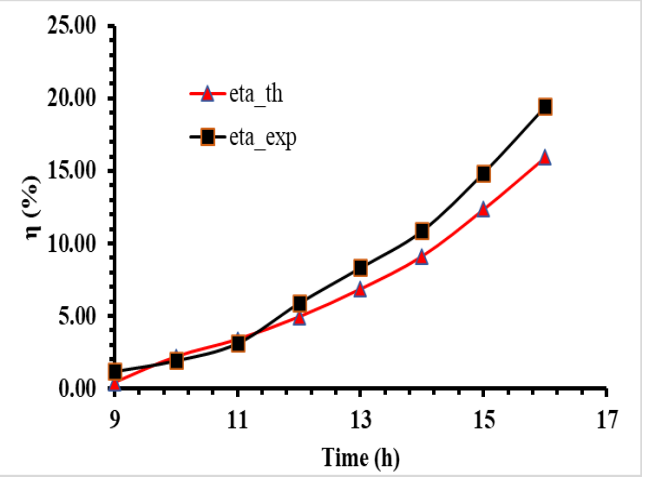

Fig. 7: Variation of instantaneous efficiency.

6. Conclusion

Water scarcity poses significant challenges worldwide, requiring innovative approaches for sustainable water provision. This study showcases the potential of Excel modelling in understanding the performance of CSS. By using Dunkle's empirical relations and VBA functions, Excel facilitates the prediction of CSS productivity and efficiency with a variation of 16 and 19%, by using Dunkle's formula, which is in accordance with the literature. Experimental validation demonstrates the efficacy of the model in capturing real-world performance. Excel's user-friendly interface and analytical capabilities make it an invaluable tool for

researchers, educators, and practitioners in addressing global water challenges. Through continued refinement and application, Excel modelling can contribute significantly to the progression in the field of sustainable water solutions.

The current study can be expanded by modelling various theoretical models to predict the distillate output of CSS by using Microsoft Excel. Moreover, a detailed Exergy analysis of the still can also be done in the future by developing the Microsoft Excel add-ins for it. Additionally, time-marching solutions, which use iterative calculations to predict water and inner glass temperatures, along with other relevant parameters (varying basin water mass, glass thickness, basin thickness, Angle of inclination of the glass, solar stills characteristic dimension, *etc*.), can be executed. This topic has substantial potential for providing deeper insights into the capabilities of Microsoft Excel and solar still modeling.

Acknowledgements
The authors are grateful to the lab staff of JUET for rendering help during experiments.

Conflict of Interest
There is no conflict of interest.

Supporting Information
Not applicable.

Nomenclature

a	Accuracy of the instrument
A_s	Surface area of water (m^2)
c_p	Specific heat at constant pressure (J/kg-K)
d	Characteristic dimension of solar still (m)
F_{12}	View factor between water and glass
F_{cw}	Convective heat transfer fraction
F_{rw}	Radiative heat transfer fraction
F_{ew}	Evaporative heat transfer fraction
g	Acceleration due to gravity (m/s^2)
Gr	Grashoff number
h_{cw}	Convective heat transfer coefficient (W/m^2-K)
h_{ew}	evaporative heat transfer coefficient (W/m^2-K)
h_{rw}	Radiative heat transfer coefficient (W/m^2-K)
h_{1w}	Overall heat transfer coefficient (W/m^2-K)
I	Solar radiation intensity (W/m^2)
k	Thermal conductivity (W/m-K)
L	Latent heat (J/kg)
$\dot{m}_{ew}$	Distillate output (kg/m2-hr)
Nu	Nusselt number
p_w	Partial saturated vapour pressure at water temperature (Pa)
p_{ci}	Partial saturated vapour pressure at inner glass temperature (Pa)
Pr	Prandtl number
q_{cw}	Convective heat transfer rate (W/m^2)
q_{ew}	evaporative heat transfer rate (W/m^2)
q_{rw}	Radiative heat transfer rate (W/m^2)
q_{1w}	Overall heat transfer rate (W/m^2)
T_w	Basin water temperature (°C)
T_{ci}	Inner condensing cover temperature (°C)
T_v	Average water temperature (°C)
u	Standard uncertainty

Greek

ρ	Moist air density (kg/m^3)
μ	Dynamic viscosity (Ns/m^2)
β	Volumetric expansivity (K^{-1})
ΔT	Water and glass temperature difference (°C)
σ	Stefan-Boltzmann constant (W/m^2-k^4)
ϵ_g	Emissivity of glass
ϵ_w	Emissivity of water

Abbreviations

CSS	Conventional solar still
HSS	Hemispherical solar stills
VBA	Visual Basic applications
FRP	Fiberglass reinforced plastic
GI	Galvanized iron

References

[1] H. Soonmin, M. Taghavi, Solar energy development: study cases in Iran and Malaysia, *International Journal of Engineering Trends and Technology*, 2022, **70**, 408-422, doi: 10.14445/22315381/ijett-v70i8p242.

[2] A. Ahmad, T. Azam, Water purification technologies, *Bottled and Packaged Water*, 2019, **4**, 83-120, doi: 10.1016/b978-0-12-815272-0.00004-0.

[3] H. Panchal, A. Awasthi, Theoretical modeling and experimental analysis of solar still integrated with evacuated tubes, *Heat and Mass Transfer*, 2017, **53**, 1943-1955, doi: 10.1007/s00231-016-1953-8.

[4] A. Awasthi, K. Kumari, H. Panchal, R. Sathyamurthy, Passive solar still: recent advancements in design and related performance, *Environmental Technology Reviews*, 2018, **7**, 235-261, doi: 10.1080/21622515.2018.1499364.

[5] H. Panchal, Y. Taamneh, R. Sathyamurthy, A. E. Kabeel, S. A. El-Agouz, P. Naveen Kumar, A. M. Manokar, T. Arunkumar, D. Mageshbabu, R. Bharathwaaj, Economic and exergy investigation of triangular pyramid solar still integrated to inclined solar still with baffles, *International Journal of Ambient Energy*, 2019, **40**, 571-576, doi: 10.1080/01430750.2017.1422143.

[6] Z. M. Omara, A. S. Abdullah, A. E. Kabeel, F. A. Essa, The cooling techniques of the solar stills' glass covers - A review, *Renewable and Sustainable Energy Reviews*, 2017, **78**, 176-193, doi: 10.1016/j.rser.2017.04.085.

[7] S. Subhani, R. S. Kumar, Numerical investigation on influence of mounting baffles in solar stills, *Renewable Energy Sources and Technologies*, 2019, **2161**, 020025, doi: 10.1063/1.5127616.

[8] D. Mevada, H. Panchal, K. K. Sadasivuni, M. Israr, M. Suresh,

S. Dharaskar, H. Thakkar, Effect of fin configuration parameters on performance of solar still: A review, *Groundwater for Sustainable Development*, 2020, **10**, 100289, doi: 10.1016/j.gsd.2019.100289.
[9] Y. Raghuvanshi, P. Dumka, D. Mishra, Modelling logic gates in Python, *International Journal for Multidisciplinary Research*, 2022, **4**, 1-8, doi: 10.36948/ijfmr.2022.v04i05.043.
[10] R.V. Dunkle, Solar water distillation, the roof type still and a multiple effect diffusion still, International Developments in Heat Transfer, Proceeding of International Heat Transfer, University of Colorado, 1961, **5**, 895.
[11] J. A. Clark, The steady-state performance of a solar still, *Solar Energy*, 1990, **44**, 43-49, doi: 10.1016/0038-092x(90)90025-8.
[12] S. Aggarwal, G. N. Tiwari, Thermal modelling of a double condensing chamber solar still: an experimental validation, *Energy Conversion and Management*, 1999, **40**, 97-114, doi: 10.1016/s0196-8904(98)00110-1.
[13] D. B. Spalding, Convective Mass Transfer, Arnold, London, 1963.
[14] P. T. Tsilingiris, Combined heat and mass transfer analyses in solar distillation systems–The restrictive conditions and a validity range investigation, *Solar Energy*, 2012, **86**, 3288-3300, doi: 10.1016/j.solener.2012.08.009.
[15] P. T. Tsilingiris, Theoretical derivation and comparative evaluation of mass transfer coefficient modeling in solar distillation systems - the Bowens ratio approach, *Solar Energy*, 2015, **112**, 218-231, doi: 10.1016/j.solener.2014.11.021.
[16] K. Ghachem, C. Maatki, L. Kolsi, N. Alshammari, H. Oztop, M. Borjini, A. Ben, K. Al-Salem, Numerical study of heat and mass transfer optimization in a 3D inclined solar distiller, *Thermal Science*, 2017, **21**, 2469-2480, doi: 10.2298/tsci150323161g.
[17] O. Younis, A. K. Hussein, M. El Hadi Attia, H. S. S. Aljibori, L. Kolsi, H. Togun, B. Ali, A. Abderrahmane, K. Subkrajang, A. Jirawattanapanit, Comprehensive review on solar stills: latest developments and overview, *Sustainability*, 2022, **14**, 10136, doi: 10.3390/su141610136.
[18] M. El Hadi Attia, M. Shajahan, A. M. Manokar, A. K. Hussein, E. Elaloui, H. Togun, L. Kolsi, Experimental studies on the effect of nanofluid and glass cooling on the performance of hemispherical solar still: Energy and exergy approach, *Iranian Journal of Chemistry and Chemical Engineering*, 2024, **43**, 1792-1809, doi: 10.30492/ijcce.2024.1999973.5962.
[19] O. Younis, A. K. Hussein, M. El Hadi Attia, F. L. Rashid, L. Kolsi, U. Biswal, A. Abderrahmane, A. Mourad, A. Alazzam, Hemispherical solar still: recent advances and development, *Energy Reports*, 2022, **8**, 8236-8258, doi: 10.1016/j.egyr.2022.06.037.
[20] J. Ranjani, A. Sheela, K. P. Meena, Combination of NumPy, SciPy and Matplotlib/Pylab - a good alternative methodology to MATLAB - A comparative analysis, 2019 1st International Conference on Innovations in Information and Communication Technology (ICIICT), April 25-26, CHENNAI, India, IEEE, 2019, doi: 10.1109/iciict1.2019.8741475.
[21] J. M. Lindquist, C. A. Sulewski, Microsoft Excel: The universal tool of analysis, Handbook of Military and Defense Operations Research, Chapman and Hall, CRC Press, 2020, 19-54, ISBN: 9780429467219.
[22] M. Triyanto, A. Andriyati, I. Kamila, E. Rohaeti, Pemodelan pengaruh nilai tukar rupiah terhadap dollar dengan indeks harga saham gabungan kompas 100 menggunakan metode Gauss Newton, *Journal Jendela Matematika*, 2024, **2**, 1-10, doi:10.57008/jjm.v2i01.669.
[23] R. K. Tan, K. Önder, F. Yerisenoglu, R. Mutlu, Usage of an Excel spreadsheet for a thermal endurance test report, *European Journal of Applied Science, Engineering and Technology*, 2023, **3412**, 91-97, doi: 10.55581/ejeas.1398578.
[24] G. Fellah, Excel spreadsheet as a tool for simulating the performance of steam power plants, *Spreadsheets in Education* 2019, **12**, 1-19.
[25] M. Al-Awad, Modelling the regenerator for multi-objective optimisation of the air-bottoming cycle with Excel, *Spreadsheets Education*, 2016, **9**, 1-13.
[26] H. Oike, Y. Ogawa, K. Oishi, Simple and quick visualization of periodical data using Microsoft Excel, *Methods and Protocols*, 2019, **2**, 81, doi: 10.3390/mps2040081.
[27] F. W. Z. LaPolla, Excel for data visualization in academic health sciences libraries: a qualitative case study, *Journal of the Medical Library Association*, 2020, **108**, 67-75, doi: 10.5195/jmla.2020.749.
[28] J. P. Holman, B. K. Holman, What every engineer should know about Excel, CRC Press, Boca Raton, 2018, ISBN: 9781315268583.
[29] J. P. Holman, Experimental methods for engineers, McGraw-Hill, New York, 2017, ISBN: 9780071326483.
[30] R. Kumar, D. R. Mishra, P. Dumka, Improving solar still performance: A comparative analysis of conventional and honeycomb pad augmented solar stills, *Solar Energy*, 2024, **270**, 112408, doi: 10.1016/j.solener.2024.112408.
[31] S. Toyama, T. Aragaki, H. M. Salah, K. Murase, M. Sando, Simulation of a multieffect solar still and the static characteristics, *Journal of Chemical Engineering of Japan*, 1987, **20**, 473-478, doi: 10.1252/jcej.20.473.
[32] G. N. Tiwari, A. K. Tiwari, Solar distillation practice for water desalination systems, Anamaya, New Delhi, 2008, ISBN: 13978-81-88342-71-6.
[33] T. L. Bergman, A. S. Lavine, F. P. Incropera, D. P. DeWitt, Fundamentals of heat and mass transfer, John Wiley & Sons, Hoboken, 2018, ISBN: 978-1-119-35388-1.
[34] I. Mohan, S. Yadav, H. Panchal, S. Brahmbhatt, A review on solar still: a simple desalination technology to obtain potable water, *International Journal of Ambient Energy*, 2019, **40**, 335-342, doi: 10.1080/01430750.2017.1393776.
[35] G. N. Tiwari, S. A. Lawrence, New heat and mass transfer relations for a solar still, *Energy Conversion and Management*, 1991, **31**, 201-203, doi: 10.1016/0196-8904(91)90073-r.
[36] A. K. Singh, R. K. Yadav, D. Mishra, R. Prasad, L. K. Gupta, P. Kumar, Active solar distillation technology: A wide overview, *Desalination*, 2020, **493**, 114652, doi:

10.1016/j.desal.2020.114652.
[37] P. Dumka, D. R. Mishra, Experimental investigation of modified single slope solar still integrated with earth (I) &(II): Energy and exergy analysis, *Energy*, 2018, **160**, 1144-1157, doi: 10.1016/j.energy.2018.07.083.
[38] P. T. Tsilingiris, Parameters affecting the accuracy of Dunkle's model of mass transfer phenomenon at elevated temperatures, *Applied Thermal Engineering*, 2015, **75**, 203-212, doi: 10.1016/j.applthermaleng.2014.09.010.